RF-induced pinch of resonant 3He minority ions in JET

T. Johnson, T. Hellsten, M. Mantsinen, V. Kiptily, S. Sharapov et al.

Citation: AIP Conf. Proc. 595, 102 (2001); doi: 10.1063/1.1424154
View online: http://dx.doi.org/10.1063/1.1424154
View Table of Contents: http://proceedings.aip.org/dbt/dbt.jsp?KEY=APCPCS&Volume=595&Issue=1
Published by the American Institute of Physics.

RF-induced Pinch of Resonant ^{3}He Minority Ions in JET

T Johnson*, T Hellsten*†, M Mantsinen**, V Kiptily‡, S Sharapov‡, J Hedin*, J-M Noterdaeme§, M-L Mayoral‡, F Nguyen¶ and contributors to the EFDA-JET workprogram

*Alfvén Laboratory, Association EURATOM/VR, Sweden
†also EFDA Close Support Unit, Abingdon UK
**Association EURATOM/Tekes, Finland
‡Association EURATOM/UKAEA, UK
§MPI für Plasmaphysik, Association EURATOM/IPP, Germany
¶CEA Cadarache, Association EURATOM/CEA, France

Abstract. The RF-induced pinch of ^{3}He minority ions has been observed in JET affecting the diamagnetic energy, the fast ion energy content, the sawtooth period, the Alfvén eigenmode excitation and the γ-emission. Further, the γ-emission is consistent with RF-detrapping into co-current passing orbits. The results from the SELFO code are consistent with the observations.

INTRODUCTION

During ICRH high energetic anisotropic tails of resonant ions are produced [1]. The energy of the tails are determined by the balance between power absorbed by the wave field, power transfered to the background plasma and transport of the energetic ions. The latter is due to both collisional transport, and wave-particle induced transport, the so called RF-induced pinch [2]. Experimental study of the RF-induced pinch is possible by the dependence on the toroidal mode number, which can be altered by changing the phase between the currents in the antenna straps. For hydrogen minority heating the RF-induced pinch has been indirectly observed through the effect on sawtoothing, line integrated proton distribution function and triggering of Alfvén eigenmodes [3]. Further, tomografic reconstruction of γ-emission from ^{3}He ions heated with symmetric toroidal mode spectrum is consistent with an RF-induced pinch of trapped orbits and a detrapping of these orbits into co-current passing ones [4]. Here experiments are analysed by comparing the effect on the ^{3}He ions for different phasings, see also [5].

For one toroidal wave mode in the ICRF, wave-particle interactions transport the resonant ions along characteristics in the space of invariants of motion in an axisymmetric torus; energy E, magnetic moment μ (or $\Lambda = B_0\mu/E$) and canonical toroidal angular momentum P_ϕ (Fig. 1). For increasing energy, Λ approaches $\Lambda_{res} = n\omega_c/\omega$ asymptotically, corresponding to the motion of the trapped ion turning points towards the resonance (Fig. 1). The motion in P_ϕ gives rise to the RF-induced pinch, which is the motion of the trapped ion turning points across the magnetic flux surfaces. Depending on the direction of the toroidal wave propagation the pinch can transport ions outwards or inwards. If

CP595, *Radio Frequency Power in Plasmas: 14th Topical Conf.*, edited by T. K. Mau and J. deGrassie
2001 American Institute of Physics 0-7354-0038-5

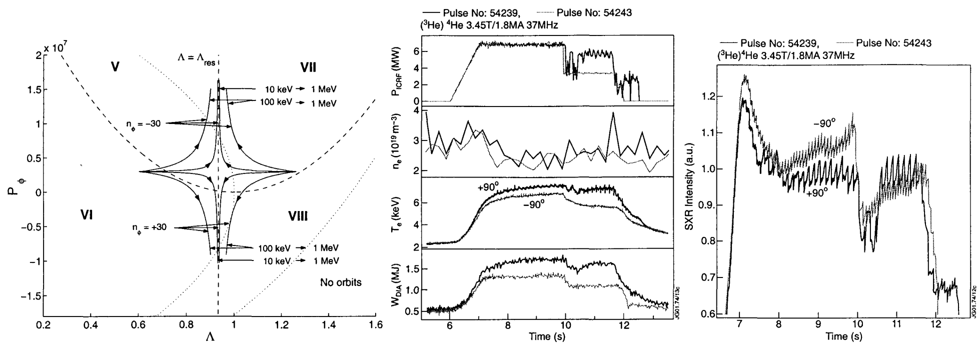

FIGURE 1. *To the left, characteristics in $(E,\Lambda,\tilde{P}_\phi)$ space projected on the $(\Lambda,\tilde{P}_\phi)$-plane, were $\tilde{P}_\phi = P_\phi/m$ [4]. In the middle, experimental parameters from JET pulse #54243 and #54239. To the right, the sawteeths behaviour measured by SXR.*

the turning points meet in the mid plane, the orbit will be detrapped into a passing one. For high energies this transition exclusively produces co-current passing orbits [6, 7]. An inward pinch is obtained when the waves propagates in the direction of the plasma current. This is the case for the 90° phasing in JET, which in Fig 1 corresponds to a negative toroidal mode number.

ANALYSIS OF EXPERIMENTAL RESULTS

Experiments have been carried out in a ^{4}He plasma with a ^{3}He minority concentration of 1-2% [5]. The cyclotron resonance was located at $R \sim 2.82m$ with $B_0 = 3.45\,T$ and $f = 37.3\,MHz$. In the pulses #54243 and #54239 with $-90°$ and $90°$ phasing, respectively, the density and ICRH power were the same up to $10\,s$, while the diamagnetic energy (Fig. 1), sawtooth behaviour (Fig. 1), TAE activity (Fig. 2) and γ emission (Fig. 3), all show clear differences between the two pulses. These pulses have been analyzed using the SELFO code [8, 9], which solves the distribution function, using the FIDO code [10], and the wave field, using the LION code [11, 12], in a self-consistent manner.

The differences in diamagnetic energy comes from the differences in thermal and fast ion energy content. Both terms are larger with 90° phasing due to the increase in confinement of energetic ions by the inward pinch, which allows for a higher tail energy, producing more power transfer to the electrons by collisions, compared to the decrease in confinement by the outward pinch. The sawtooth period is longer with 90° phasing, which is consistent with the stabilizing effect of fast ions inside the $q = 1$ surface [13]. The fast ion perpendicular energy content is calculated by SELFO to be $0.43\,MJ$ for #54239 and $0.34\,MJ$ for #54243, whereas in the experiments $\sim 0.5\,MJ$ and $\sim 0.3\,MJ$ were measured, respectively. The discrepancy in the differences between the two pulses is probably caused by wall losses in the simulation of #54239 that prohibits the long time scale detrapping into co-current passing orbits to reach steady state.

In order to excite Alfvén eigenmodes a sufficiently strong radial gradient of fast ions satisfying the resonance conditions is required [14]. In pulse #54239 both TAE and EAE modes were observed while no AE modes were observed #54243, which is consistent with the larger pressure gradient in #54239 calculated with the SELFO code (Fig. 2).

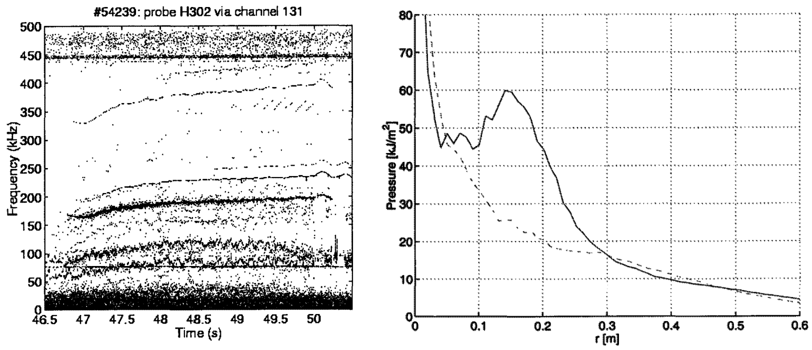

FIGURE 2. *The two figures to the left shows AE modes in pulse* #54243 *and* #54243. *TAE's are at* 150-250*kHz and EAE's are at* 325-450*kHz. To the right, the pressure of resonant ions calculated with SELFO for pulse* #54243 *(solid line) and* #54243 *(dashed line).*

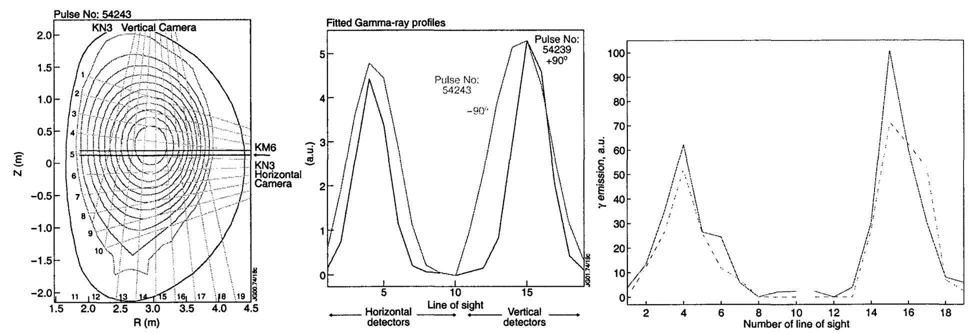

FIGURE 3. *To the left the lines of sight though the poloidal cross section [15]. In the middle, the measured* γ*-emission in pulse* #54239 *and* #54243. *To the right, the measured* γ*-emission in pulse* #54081. *The magnitude of the emission in* #54243 *is normalized by a factor* 4.7 *compared to* #54239. *The cyclotron resonances is located around channel* 14 *in all pulses.*

The emission of γ's from $^{12}C(^3He,p\gamma)^{14}N$ reactions has been measured with 19 lines of sight spanning a mesh over the poloidal cross section (Fig. 3). The measured γ's in #54243 are consistent with an energetic population of trapped ions with their turning point close to the cyclotron resonance, channel 13 and 14. These ions also produce γ's on the LFS, channel 15, 16, ..., but the intensity decreases with increasing $|v_{\parallel}(R)| = \sqrt{1 - B(R)\mu/E}$. In the simulation 79 % of the ions with energies above $2MeV$ were trapped, (Fig. 4). In pulse #54239 the γ-emission was stronger and shifted towards the LFS. This is consistent with the increased confinement of energetic ions and the RF-induced detrapping into co-current passing orbits that are shifted towards the LFS by the ∇B and curvature drift [4]. For this pulse the simulations produced more ions above $2MeV$ than in #54243, and 73 % of them were passing, (Fig. 4). Among ions above $500keV$, ~ 50 % were passing for both pulses. This is due to a combination of the sub dominant component of the toroidal mode spectra that produces an outward pinch for a subset of the distribution function in #54239 (Fig. 4) [4], and the Doppler shifted

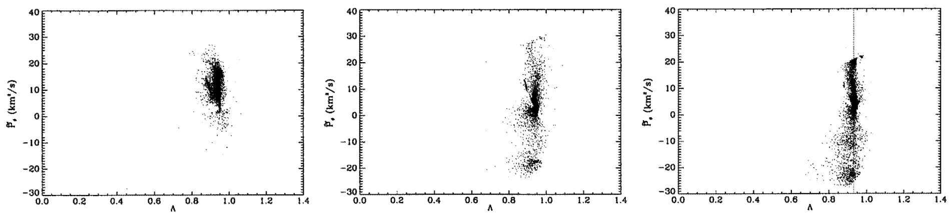

FIGURE 4. *The distribution function of* 2-5 MeV ^{3}*He ions calculated with SELFO for pulse* #54243 *(left),* #54239 *(middle) and* #54081 *(right), compare with Fig. 1. For* $P_\phi < 0$ *only co-current orbits exists.*

absorption that reduces the wave field strength at the resonance and thereby reducing the absorption by ions with smaller Doppler shift [9].

Similar γ-emission profiles as in #54239 have also been observed in a reversed shear plasma with an internal transport barrier, #54081 (Fig. 3), with 90° phasing ($B_0 = 3.42T$, $f = 37.4MHz$, $n_e = 2.6 \times 10^{19} m^{-3}$ and $T_e = 7keV$). Due to the very low concentration of reminiscent ^{3}He ions the power per particle and the energy of the tail is higher, and the RF-induced detrapping becomes stronger than in #54239 (Fig. 4).

CONCLUSIONS

The RF-induced inch has been observed in the differences between pulses with 90° and −90° antenna phasing. The diamagnetic energy, fast ion energy content and sawtooth period indicate a significant increase in the confinement of fast ions with 90° phasing. Both EAE and TAE modes were observed with 90° phasing, but neither were observed with −90° phasing. The γ-emission is shifted towards the LFS by the RF-induced detrapping into co-current passing orbits. Simulations with the SELFO code reproduces the measured perpendicular fast ion energy content, produces differences in the ion pressure gradients for the two phasing consistent with measured TAE and EAE emission, and produces RF-induced detrapping into co-current passing orbits consistent with measured γ-emission.

REFERENCES

1. T.H. Stix, *Nuclear Fusion*, **15** 737–754 (1975)
2. L. Chen, J. Vaclavik, and G.W. Hammett, *Nuclear Fusion*, **28** 389 (1988)
3. L.-G. Eriksson et al., *Physical Review Letters*, **81** 1231–1234 (1998)
4. J. Hedin, et al., *To appear in Nuclear Fusion*, (2001)
5. M. Mantsinen et al., (at this conference)
6. I. Furno et al., *22st EPS Conference on Controlled Fusion and Plasma Phys.*, **II** 253 (1995)
7. J. Carlsson, T. Hellsten, and J. Hedin, *Physics of Plasmas*, **5** 2885–2892 (1998)
8. J. Hedin, T. Hellsten, and J. Carlsson, In *Theory of Fusion Plasmas 1998*, page 467, (1999)
9. J. Hedin, T. Hellsten, and L.-G. Eriksson, *Nuclear Fusion*, **40** 1819 (2000)
10. J. Carlsson et al., In *Proc. of the Joint Varenna-Lausanne Workshop*, page 351, (1994)
11. L. Villard, et al., *Computer Physics Reports*, **4** 95 (1986)
12. L. Villard, S. Brunner, and J. Vaclavik, *Nuclear Fusion*, **35** 1173 (1995)
13. F. Porcelli, *Plasmas Physics and Controlled Nuclear Fusion*, **33** 1601 (1991)
14. H. Biglari, F. Zonca, and L. Chen, *Phys. Fluids*, 2385 (1992)
15. J.M. Adams et al., *Nucl. Instrum. Methods Phys. Res.*, 277 (1993)